Air-Source Heat Pump with Integrated Latent Heat Storage for Residential Buildings: Concept Development and Design Evaluation

Arash Bastani(✉) and Justin Tamasauskas

CanmetENERGY, Natural Resources Canada, Varennes, QC, Canada
arash.bastani@nrcan-rncan.gc.ca

Abstract. Heat pumps effectively support electrification and reduce energy consumption associated with building heating and cooling. Air-source heat pumps (ASHP) use the ambient air as a thermal source or sink for the heat pump (HP). ASHPs are the most common form of HP system in Canadian residential buildings due to their simplicity and lower initial cost. While the technology is recognized to play a key role in the path to building decarbonization, its widespread adoption will significantly increase peak demand for electricity grids, especially in regions where fossil fuel-based systems are to be replaced. Thermal storage technology can support the increased adoption of ASHPs in those regions by providing a more energy-flexible link between the building's thermal demand and the electrical grid.

This study investigates a new method of integrating and applying a phase change material (PCM) as latent heat storage in an ASHP system for residential buildings. The approach employs direct heat exchange between the refrigerant and the PCM and indirect discharge of thermal energy into the room. This research describes the concept and evaluates its advantages. It also explores two suggested design configurations to integrate the storage unit into current ASHP systems. This research further evaluates the effect of those configurations on the storage unit's charging process via a numerical model developed to simulate heat transfer in the storage medium.

Keywords: Air-Source Heat Pump · PCM thermal storage · refrigerant/PCM heat exchanger · Thermal Storage for both heating and cooling

1 Introduction

The building sector accounts for a significant portion of total energy use in Canada, with a large percentage of this energy use dedicated to space heating and cooling. The built environment is thus associated with greenhouse gas (GHG) emissions and other environmental issues. Addressing this issue calls for a broader effort to integrate renewable energy sources and energy-efficient heating and cooling systems.

Heat pumping technology effectively supports electrification, reduces energy consumption associated with building heating and cooling, and reduces annual GHG emissions when coupled with grid decarbonization. Air-source heat pumps (ASHP) use the

P. Schossig et al. (Eds.): IRES 2022, AHE 16, pp. 29–46, 2023.
https://doi.org/10.2991/978-94-6463-156-2_4

ambient air as a thermal source (in heating) or thermal sink (in cooling). ASHPs are the most popular form of heat pump integration in Canada due to their relative installation simplicity, low initial cost, and environmentally friendly features. Nonetheless, ASHP adoption causes some challenges, as described here.

i. Increasing demand on the electric grid during peak hours:
   A growth in HP adoption can significantly increase peak demand for electricity grids, particularly in regions that currently use natural gas heating. This leads to dispatching backup generators (often fossil-fuel-based generators), which increases GHG emissions and electricity production costs. In addition, many electricity grids have limited additional free capacity during peak hours. This effectively limits the number of heat pumps that can be installed in a given region or requires a significant investment and expansion of grid infrastructure to support the added demand.
ii. Reduced capacity and performance during extremely low or high ambient temperature days:
   An ASHP suffers from decreased capacity and performance during extremely low or high ambient temperature days. During very hot or cold times of the year, the compressor operates with an increased pressure ratio to inject or extract heat from the outdoor air. In that situation, the capacity and efficiency of the ASHP may drop significantly. In cold climate regions, when the ambient temperature is below the ASHP's minimum operating temperature, the HP is shut down and replaced by an auxiliary heater (a fossil-fuel-based system or a much less efficient electrical heater). Moreover, the compression cycle needs to be reversed frequently to avoid the accumulation of frost on the outdoor heat exchanger, which not only stops heating the room but also adds some heating load by operating the indoor unit as an evaporator. Other defrost mechanisms, e.g., an electrical coil, and the hot gas bypass are energy-intensive too.

HPs accompanied with thermal energy storage (TES) can support the grid and provide flexibility during electrical peak demand hours by decoupling thermal energy generation and demand. They use electricity to provide thermal energy during off-peak hours, which can be stored and used to condition the home during a period of higher electricity demand. Amongst thermal storage mediums, phase change materials (PCMs) attract the interest of researchers since they take advantage of the high energy density of the latent heat through the freezing and melting process. Thus,

- latent heat storages yield a reduction in the size of the storage unit compared to the sensible TES system
- PCMs offer more stable storage temperatures during the thermal energy charging and discharging processes

This means generally lower thermal losses and more consistent and higher performance of the accompanying heat pump (HP). Thus, PCMs have gained more attention from researchers to be coupled with HPs in the past two decades. Moreno et al. [1] and Pardinas et al. [2] reviewed different approaches to integrating PCM storage units

into HP systems. With the focus on heating applications, presently, the following concepts integrate PCMs into ASHPs to improve demand flexibility and HPs' performance, particularly in cold climate regions.

a. PCMs connected to the condenser (Direct discharge to the room):

   This concept directly employs PCMs for space heating, which is melted by the HP condenser during off-peak hours. It mainly aims to store thermal energy and shift the electrical demand for space heating to off-peak periods. A part or total condenser's capacity heats the TES during off-peak periods and charges the TES. During peak hours, the ASHP stops working, and the stored heat in the PCM is used to condition the room. Agyenim and Hewitt [3] investigated this approach to potentially meet the total residential heating energy load for common buildings in the UK. Maaraoui et al. [4] developed a numerical model to properly design the PCM/air heat exchanger connected to an air-to-air HP.

   While it is the easiest method to integrate a PCM into an ASHP with minimal modifications, the TES unit must be large enough to address the entire heating load during peak hours. This would be challenging for places with limited free space to add a TES unit. The design rationale also limits the selection of PCMs with certain melting temperatures. For instance, PCMs with melting temperatures above 40 °C are required to address heating load. This specification requires the compressor to operate above a certain discharge pressure to provide the required temperature difference to melt the PCM. In addition, the TES unit is dedicated only to a single operational mode of the ASHP; here, it is only the heating mode. The TES with a melting temperature above 40 °C does not contribute to the cooling operation.

b. PCMs to improve the defrosting process in ASHPs:

   This approach targets improving the performance of ASHPs by shortening the defrosting process and reducing its impact on the heating load. Instead of reversing the HP cycle or using an electrical heater, this approach uses PCM to defrost the outdoor coil. The surplus of the condenser heats PCMs and melts the storage material. When defrosting is needed, the HP reverses the cycle and extracts heat from the PCM instead of the indoor space. Dong et al. [5] experimentally compared defrosting with a PCM storage with the conventional reverse-cycle defrosting in an ASHP with a nominal 2.5 kW heating capacity. They demonstrated that PCM storage reduces the defrosting period and energy consumption by 60% and 48%, respectively. Minglu et al. [6] also experimentally evaluated the use of PCM storage for a defrosting application. They concluded that a shorter defrosting period and a higher indoor air temperature supply help improve the indoor thermal comfort during the defrosting period.

While this approach improves the defrosting process and eventually the heating efficiency of an ASHP, it does not necessarily provide flexibility to an electrical grid. Concerning the increased load on the grid, the storage needs to be designed to shave or remove electrical loads during peak hours.

This paper introduces a new approach for integrating a thermal storage unit into an ASHP (ASHP + Storage) and describes two possible design configurations of this approach. The charging process of the storage unit depends on the design configuration and the thermal load of the building. Therefore, the focus of this study is only on the numerical evaluation of the charging process during the heating season.

2 Approach to Integrating a PCM Storage Unit into an ASHP

2.1 Conceptualization of the Approach:

A new approach is studied to integrate a PCM into an ASHP in order to address the drawbacks of the current methods presented in the previous section. The design of the proposed system includes a focus on:

a. *Compact storage design*: Space is at a premium in residential buildings. This proposed system uses latent thermal storage, taking advantage of higher energy densities to minimize storage volumes.
b. *Flexible operation*: This proposed system avoids limiting the operating pressure of an ASHP's compressor by selecting PCMs with lower melting temperatures.
c. *Suitability*: ASHPs are the most common HP integration in Canada due to their simplicity and lower cost. The proposed system targets the integration of thermal storage with air-air HPs, and supplements both *heating and cooling* applications.

The system's concept is shown in Fig. 1 for heating applications and consists primarily of:

i. An evaporator, which is used to extract thermal energy from the air outdoors (heating application) or within an indoor space (cooling application);
ii. A condenser, which is used to reject thermal energy to the air within an indoor space (heating application) or outdoors (cooling application);
iii. A thermal storage unit, which consists of refrigerant pipes surrounded by a PCM. Thermal energy is transferred to/from the storage by circulating all or a portion of refrigerant from the HP cycle through the pipes of the storage unit. This unit stores thermal energy at a temperature close to room temperature (~20 °C), which replaces the ambient air on the source side of the ASHP and provides a smaller temperature lift during the discharging mode.

The new proposed system includes an additional component (the storage unit) that acts as an additional sink or source of thermal energy for the HP. Regarding the storage unit, two principle actions exist. In the heating season, the actions are:

a. Adding thermal energy to the storage unit (charging mode): In charging mode, the refrigerant that would (in a conventional ASHP) only pass through the condenser also passes through the storage unit. This refrigerant then rejects its thermal energy to the storage material, meaning that a portion of the condenser's capacity is used to melt the PCM instead of heating the room. This creates a direct heat exchange between the two-phase refrigerant and the storage medium. Depending on the thermal load of the building during the charging process, a part or total capacity of the ASHP may be used to charge the TES unit.
b. Removing thermal energy from the storage unit (discharging mode): In discharging mode, the evaporator is bypassed, and the storage is used as a source for the HP. Cool refrigerant passes through the storage unit and extracts stored thermal energy. This refrigerant then passes through the compressor, where its pressure and temperature are raised, before rejecting its thermal energy at the condenser. In fact, the stored thermal energy is discharged indirectly into the room.

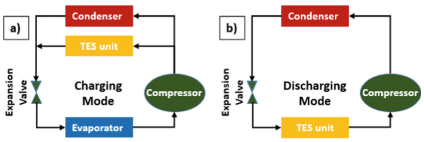

Fig. 1. Basic ASHP + Storage system concept diagram for heating application a) Charging mode; b) Discharging mode

2.2 System Configurations and Operating Modes:

The proposed ASHP + Storage system can supplement heating and cooling operations by using a PCM with a melting temperature close to the room temperature (~20 °C), as described below. It should be noted that in cooling mode, the evaporator and condenser reverse locations (i.e., the evaporator is now located inside the space). To maintain a consistent terminology for both operational modes, this section uses the terms indoor unit and outdoor unit to refer to the heat exchangers located inside and outside the building, respectively. Two configurations have been proposed to integrate the storage unit into the vapor compression cycle: series and parallel. In the series configuration, the storage unit is located downstream of the indoor unit. The refrigerant that flows out of the indoor unit is used to charge the storage unit. In the latter configuration, however, the storage unit is located parallel to the indoor unit. Thus, the refrigerant is branched into two lines and flows simultaneously toward the indoor and storage units.

2.2.1 Heating Season

The series and parallel configuration schematics of the heating mode are provided in Fig. 2 and Fig. 3, respectively. During the heating season, thermal energy may be transferred to the storage (charging) during periods of low electrical demand on the grid, when building heating demand is less than the total available capacity of the heat pump. Then, during periods of higher demand on the grid, the storage may be used as a source for the heat pump in a discharge mode. This offers improved system efficiencies and lower electrical demand by providing a much warmer source temperature (~20 °C) to the heat pump vs. the outdoor air (down to −25 °C). Moreover, the storage unit can be sized with a smaller capacity than the thermal demand in the building as its discharged heat is boosted by using the work of the compressor.

2.2.2 Cooling Season

In cooling mode, the storage can represent a colder heat sink for the heat pump vs. the outdoor air. Much like in heating mode, this reduces electrical demand from the heat pump and improves system efficiencies. The series and parallel configurations schematics of the cooling mode are provided in Fig. 4 and Fig. 5, respectively.

To prepare the storage for use, thermal energy is removed from the storage during periods when cooling demand in the building is less than the total available capacity of the unit. This may be accomplished by using the storage as a secondary evaporator in the system, with thermal energy then rejected to the ambient air via the outdoor unit. During

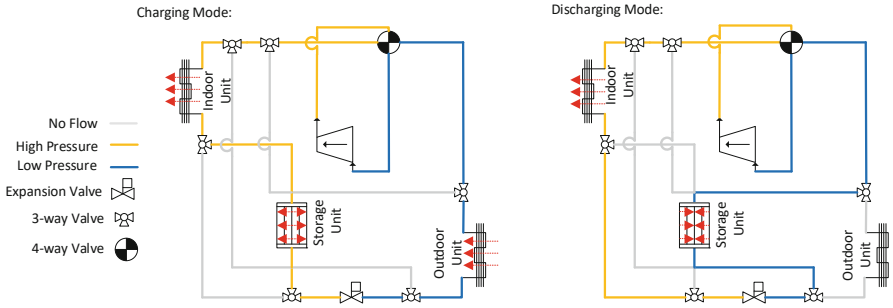

Fig. 2. System with series configuration operating in heating mode

the peak demand period, the outdoor heat exchanger is bypassed, and the heat pump rejects all its thermal energy to the storage instead of the outdoor air. This reduces the temperature difference that the heat pump must overcome, greatly improving efficiency and reducing peak demand.

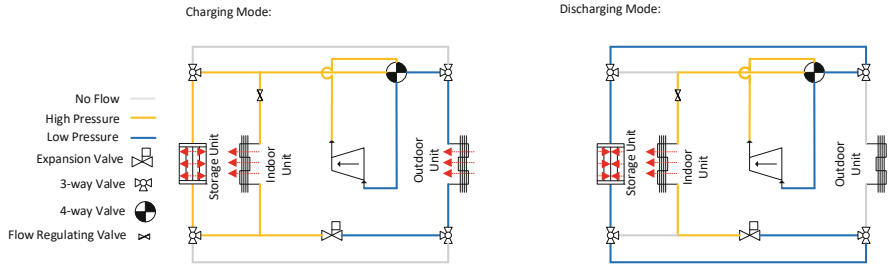

Fig. 3. System with parallel configuration operating in heating mode

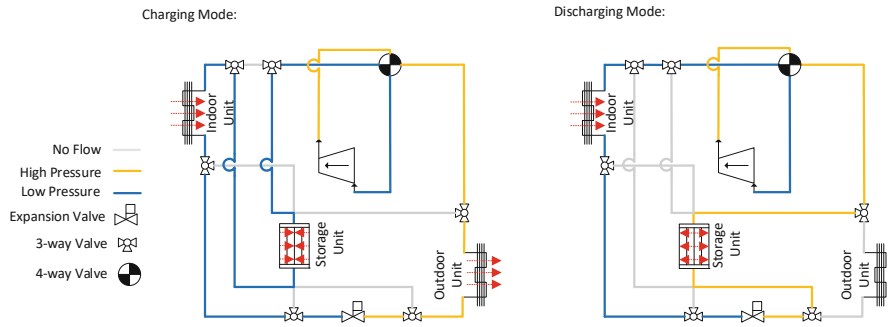

Fig. 4. System with series configuration operating in cooling mode

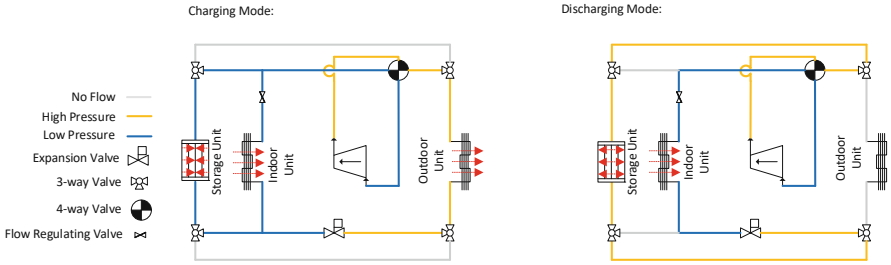

Fig. 5. System with parallel configuration operating in cooling mode

3 Model Development and Case Study

3.1 Refrigerant/PCM Heat Exchanger Model

The model proposed in this study aims to simulate the PCM storage unit integrated with an ASHP. The storage unit resembles a pipe-in-pipe heat exchanger (HX) consisting of pipes circulating the refrigerant (in this study R410a is assumed as the HP's refrigerant). The refrigerant pipe is located inside a bigger pipe that works as a sleeve. This sleeve contains a PCM and keeps it around the refrigerant pipe. Together they shape a pipe-in-pipe HX, which directly exchanges heat between the PCM and the refrigerant. The transient HX model is developed in MATLAB, based on the thermal resistance and capacitance approach (TRCA). The refrigerant inlet conditions (boundary conditions) to the heat exchanger are fixed and calculated using the CoolPack software [7]. The TRCA network of the HX is presented in Fig. 6. This shows that the pipe and its surrounding PCM are divided into a number of segments. Each segment has three nodes representing the control volume of the refrigerant (inside the inner pipe), the pipe (inner pipe thickness), and the PCM (annular section) in that segment. The segments are connected horizontally through the refrigerant nodes, accounting for its horizontal flow. The nodes in each segment come with a capacitance that accounts for their thermal mass. The resistance connecting the nodes accounts for the thermal resistance between the control volumes. The model's assumptions are:

- One directional heat transfer between the refrigerant and the PCM
- Uniform thermo-physical properties at each control volume
- No conduction and viscous dissipation in the refrigerant
- One directional flow in the refrigerant side
- No pressure drop in the fluid
- No buoyancy-based flow for liquid PCM
- No super cooling effect in the PCM

The model uses the enthalpy formulation to simplify the phase-change problem in the refrigerant and, particularly, in the PCM by avoiding the numerical instabilities involved in tracking the two-phase zone boundary [8].

The heat balance equation for the refrigerant node in the nth segment is given in Eq. (1).

$$V_{ref.,n} \times \rho_{ref.,n} \times \frac{dH_{ref.,n}}{dt} = \frac{T_{pipe,n} - T_{ref.,n}}{R_{pr,n}} + \dot{m}_{ref} \times [H_{ref.,n-1} - H_{ref.,n}] \quad (1)$$

where V is the volume [m^3] of the refrigerant control volume represented by node n, ρ is the density [kg/m^3], H is the enthalpy [J/kg], t is time [s], T is temperature [K], and $\dot{m}$ is the mass flow rate [kg/s]. $R_{pr,n}$ is the thermal resistance [K/W] between the nth refrigerant node and the nth pipe node as presented in Eq. (2).

$$R_{pr,n} = (h_{ref.,n} \times P_i \times \Delta x_n)^{-1} + \frac{\ln \frac{r_o}{r_i}}{2 \times \pi \times k_{pipe} \times \Delta x_n} \quad (2)$$

where h_{ref} is the convective heat transfer coefficient [W/m^2-K] of the refrigerant, P_i is the inner perimeter [m] of the inner pipe, Δx is the length [m] of the nth control volume, r_o is the outer radius of the inner pipe, r_i is the inner radius of the inner pipe, and k_{pipe} is the thermal conductivity [W/m-K] of the pipe.

The first term on the right side of Eq. (1) represents the heat transfer rate between the outer surface of the inner pipe and the refrigerant. The second term accounts for the advection heat transfer in the pipe. The thermo-physical properties of the refrigerant in regards to its enthalpy and pressure are obtained by linking MATLAB code to the REFPROP software [9].

The governing equation on the PCM node is also based on the enthalpy formulation:

$$V_{PCM,n} \times \rho_{PCM,n} \times \frac{dH_{PCM,n}}{dt} = \frac{T_{pipe,n} - T_{PCM,n}}{R_{PCM}} \quad (3)$$

where R_{PCM} is the thermal resistance [K/W] between the pipe node and the PCM node as presented in Eq. (4).

$$R_{PCM,n} = \frac{\ln \frac{r_{i,o}}{r_o}}{2 \times \pi \times k_{PCM,n} \times \Delta x_n} \quad (4)$$

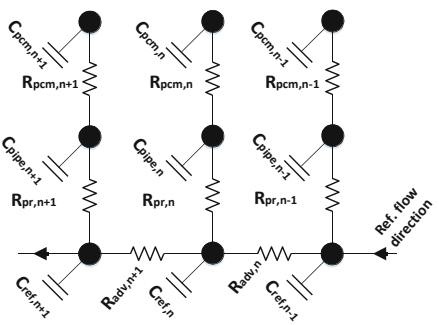

Fig. 6. TRCA network of the PCM/refrigerant HX

where $r_{i,o}$ is the inner radius of the outer pipe and k_{PCM} is the thermal conductivity of the PCM. The relationship between the temperature and the enthalpy of the PCM is presented in Eq. (5).

$$T_{PCM} = \begin{cases} \frac{H_{PCM}}{Cp_s} + T_{melt,b} & H_{PCM} < 0 \\ LF_{PCM} \times \Delta T_{melt} + T_{melt,b} & 0 \leq H_{PCM} \leq Lat_{PCM} \\ \frac{(H_{PCM} - Lat_{PCM})}{Cp_l} + T_{melt,e} & H_{PCM} > Lat_{PCM} \end{cases} \quad (5)$$

where Lat_{PCM} is the latent heat of the PCM [J/kg], $C_{p,s}$ and $C_{p,l}$ are its solid phase and liquid phase heat capacities [J/kg-K], respectively. $T_{melt,b}$ and $T_{melt,e}$ are the beginning and the end temperature [K] of the phase-change process, respectively. Their difference gives the melting range (ΔT_{melt}). Finally, LF_{PCM} is the liquid fraction calculated as below:

$$LF_{PCM} = \begin{cases} 0 & H_{PCM} < 0 \\ \frac{H_{PCM}}{Lat_{PCM}} & 0 \leq H_{PCM} \leq Lat_{PCM} \\ 1 & H_{PCM} > Lat_{PCM} \end{cases} \quad (6)$$

It should be noted that all the thermo-physical properties of the PCM are assumed to change linearly as a function of its liquid fraction during the phase change process. They stay constant, however, when the material is in its fully solid or fully liquid states.

The heat balance equation on the pipe node is based on temperature formulation:

$$V_{pipe,n} \times \rho_{pipe,n} \times Cp_{pipe,n} \times \frac{dT_{pipe,n}}{dt} = \frac{T_{ref.,n} - T_{pipe,n}}{R_{pr,n}} + \frac{T_{PCM,n} - T_{pipe,n}}{R_{PCM,n}} \quad (7)$$

where C_p is the heat capacity [J/kg-K].

The abovementioned set of differential equations is solved in a MATLAB code script and using ODE15s function. This implementation allows computing T and H at every node and time step. To ensure a high resolution of the solution, a maximum step size of 60 s is set.

3.2 Case Study

Any ASHP + Storage system should have sufficient storage capacity to reduce HP electricity use during a given peak demand event. The size of storage required to cover such a peak event is closely tied to the location and building type examined. This section presents the method used to size the storage system in the case study.

3.2.1 Building Description

In this case study, a detailed TRNSYS model of a single family home in Montreal, QC is used to determine an appropriate storage size. The selected home is based on the Canadian Centre for Housing Technology test home, and consists of two above ground floors and a finished basement with a total heated floor area of 280 m^2 [10]. Envelope performance is selected to represent typical new construction, per the National Building Code of Canada (NBC) minimum requirements for Montreal, Quebec [11]. Further details on the housing model are available in Kegel et al. [12].

3.2.2 Sizing Approach

The thermal storage is sized to cover the maximum heating demand of the home over a two-hour peak period in the winter months, ensuring to have a reasonable size of the unit. For analysis purposes, peak periods were defined as occurring either during the morning (6 AM to 9 AM), or evening hours (4 PM to 8 PM) when lighting, equipment and (in some cases) hot water use is highest [13].

The resulting simulation yields a design storage capacity of 15 kWh on the demand (building) side. It is important to note that this storage capacity will vary depending on the location and building type examined. Flexible approaches to storage size are likely required as this technology achieves a more widespread deployment.

3.2.3 Storage Unit Description

As explained in Sect. 2, the same storage unit serves the ASHP for both its heating and cooling operations. Thus, the selected PCM with a melting temperature close to room temperature (~20 °C) will be suitable for both applications. Moreover, it has a minimum heat loss, as the storage unit is located inside the building. In this case study, a salt hydrate PCM with a melting temperature ranging between 19–20 °C is selected. Its thermo- physical properties are summarized in Table 1.

For this study, the storage unit consists of three 16 m pipes circulating the refrigerant and surrounded by the PCM in their annular sections. The inner pipe has 6 mm and 8 mm inner and outer diameters, respectively. The outer pipe has a 60 mm internal diameter. Considering these dimensions, the storage unit has 11.1 kWh thermal capacity assuming its whole latent heat storage, and represents the storage capacity on the *source* side of the HP. When factoring in HP operation, this equates to 15 kWh on the *demand* (building) side of the system. From the physical appearance point of view, the storage unit may look like a box with the dimensions of 1 m (h) × 1.04 m (l) × 0.22 m (w) and a volume of 230 L.

Table 1. PCM thermo-physical properties

Properties	Magnitude
T_{melt} [°C]	19–20
Density [kg/m^3]	1530
Lat_{PCM} [kJ/kg]	195
C_p [kJ/kg-K]	2.2
$^+k_{PCM,s}$ / $k_{PCM,\ell}$ [W/m-K]	0.5 / 0.7
$^+$ s: solid state, ℓ: liquid state	

4 Results and Discussion

4.1 ASHP Simulation

The simulated ASHP is used to charge the storage unit and address the heating demand in the building. It uses R410a refrigerant as the working fluid. It is sized to provide 7.5 kW heating with its nominal compressor speed at 50 °C ($P_{sat}|_{@50\,°C} = 3063$ kPa) and − 30 °C ($P_{sat}|_{@-30\,°C} = 269$ kPa) condensation and evaporation temperatures, respectively. The ASHP is simulated at those conditions with CoolPack software to calculate the refrigerant's enthalpy, temperature, pressure, and mass flow rate at different stages of this vapor-compression cycle. It is assumed that the compressor has 70% isentropic efficiency. Figure 7 presents the pressure-enthalpy diagram of the simulated ASHP. Point 1 presents the state of the refrigerant at the discharge of the compressor. Point 2 is the outlet of the condenser with a 3 °C subcooled temperature. The isenthalpic expansion occurs between Point 2 and Point 3. Finally, the refrigerant evaporates between Point 3 and Point 4 and flows to the suction side of the compressor at a 5 °C superheated temperature.

4.2 Charging the Storage with No Heating Demand in the Building

The charging process of the storage unit is investigated on the occasions when there is no heating demand in the building. Thus, the indoor unit does not operate, and the ASHP devotes the entire heating capacity to melting the PCM. As expected, both series and parallel configurations have the same charging performance when there is no heating demand in the building: all refrigerant enters the storage unit with conditions similar to the discharge of the compressor. The developed model simulates the charging process and calculates the time required to fully charge the unit. Here, a fully-charged state means the stored thermal energy is equivalent to the storage designed capacity of 11.1 kWh. The storage is assumed to be initially at 19 °C (starting the melting process). Using the ASHP operating as presented in Fig. 7, it takes 221 min. (3 h 41 min) to fully charge the storage unit. During the charging period, the heat transfer rate to the PCM varies from 2.68 kW to 3.13 kW, with an average of 2.94 kW. It implies that the ASHP cannot use its entire heating capacity due to the low thermal conductivity of the PCM. The heat transfer rate is a function of the convective heat transfer coefficient of the refrigerant, the thermal conductivity of the PCM, the refrigerant mass flow rate, the heating surface area, and the temperature difference between the refrigerant and the PCM. Considering the convective heat transfer coefficient of the refrigerant, its thermal resistance spans between 11.4 [K-m/kW] and 44.0 [K-m/kW], while the PCM's ranges an order of magnitude higher (458 to 642 [K-m/kW]). Due to its low thermal conductivity, the thermal resistance of the PCM governs the heat transfer rate to the storage and, consequently, the heating capacity of the ASHP. Reducing the compressor speed would be a viable option to avoid cycling of the ASHP to charge the storage unit. Moreover, the proposed concept allows for reducing the discharge pressure of the compressor, as the selected PCM has a melting temperature of around 20 °C. The latter action is not feasible for conventional ASHP + storage systems that store thermal energy at temperatures above 40 °C.

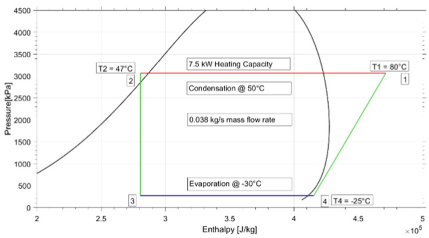

Fig. 7. P-H diagram of the simulated ASHP

The effect of reducing the compressor speed and the condensation temperature on the charging process of the storage unit is evaluated for the occasions with no heating demand in the building. Table 2 tabulates the specifications of the simulated cases. While Case 1 uses the nominal speed of the compressor, Case 2 and Case 3 are working with a reduced speed to adjust the mass flow rate, and consequently, the heating capacity of the ASHP to match the heat transfer rate of the storage unit. Moreover, in Case 3, the condensation temperature is reduced to 40 °C. The refrigerant mass flow rate is reduced significantly in Case 2 and Case 3, which are 60% and 74% lower than Case 1, respectively.

Figure 8 compares the storage heat transfer rate and the work of the compressor of those three simulated cases. In this study, the work of the compressor is calculated based on the change in the refrigerant's enthalpy across the compressor, using the following equation:

$$W_{comp.} = \dot{m}_{ref.} \times (H_{dis.} - H_{suc.}) \tag{8}$$

where $H_{dis.}$ and $H_{suc.}$ are the refrigerant's enthalpy at the discharge and the suction of the compressor, respectively. As expected, the work of the compressor is reduced in Case 2 and Case 3 with a lower refrigerant mass flow rate. In both cases, the convective heat transfer coefficient of the refrigerant is lower than in Case 1, with a higher mass flow rate. Moreover, in Case 3, the temperature difference between the refrigerant and the PCM is reduced with a lower condensation temperature. Thus, the heat transfer rate decreased by 11% and 41% in Case 2 and Case 3, respectively. Consecutively, they have 28 min. and 151 min. longer charging period than Case 1.

Table 2. Specifications of the cases with no heating demand

Simulated Cases	Nominal Compressor Speed	Condensation T [°C]	ṁ [kg/s]	Charging period [min.]
Case 1	Yes	50	0.038	221
Case 2	No<	50	0.015	249
Case 3	No<	40	0.010	372

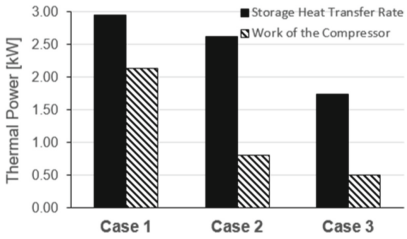

Fig. 8. Simulated cases with no heating demand in the building

4.3 Charging the Storage with Heating Demand in the Building

The charging process of the storage unit is investigated on the occasions when the building has some heating demands. Thus, the ASHP utilizes its heating capacity to serve the heating load in the building and melt the PCM in the storage unit simultaneously. On these occasions, the system configuration (series or parallel) affects the charging process of the storage unit. In the series configuration, the outlet of the indoor unit flows to the storage unit. Thus, the refrigerant stream has different thermodynamic conditions than the discharge of the compressor due to the heat exchange that occurs in the indoor unit. In the parallel configuration, however, the refrigerant stream at the inlet of the storage unit has the same thermodynamic properties as the discharge of the compressor, except for the mass flow rate. The refrigerant flow is divided into two streams: one serves the building load in the indoor unit, and the other flows to the storage unit to melt the PCM. The percentage of the refrigerant that flows to the storage unit depends on the heating load in the building. In this study, two cases are simulated assuming that the building has 60% of its peak heating load: Case 4 for a system with a series configuration, and Case 5 for a system with a parallel configuration. The specifications of these simulated cases are presented in Table 3.

In Case 5, the refrigerant mass flow rate to the storage unit is 40% of the total mass flow rate. As it is assumed that the ASHP is sized to meet the full heating load of the building, the other 60% of the refrigerant is sufficient for the indoor heating load. Table 3 indicates that Case 4 with series configuration has a lower heat transfer rate, and eventually, a longer charging period than Case 5 with parallel configuration. Like in Case 1, Case 5 uses hot gas at the discharge temperature of the compressor to melt the PCM, while two-phase R410a at 50 °C enters the storage unit in Case 4. Thus, the higher temperature difference accelerates the charging process in the parallel configuration. Case 4 and Case 5 have a lower heat transfer rate to the storage than Case 1 with no heating load in the building, though the difference is not too significant to increase the charging period substantially. As mentioned in Sect. 4.2, the low thermal conductivity of the PCM governs mainly the heat transfer phenomena in the storage unit, while the refrigerant mass flow rate and its thermal convection coefficient have less impact on the heat transfer rate. In Case 4 and Case 5, the heat transfer rate to the storage unit is only 14% and 11% lower than in Case 1. Therefore, in Case 4 and Case 5 with 4.5 kW of heating load in the building, the charging period is only 38 min. and 27 min. longer than in Case 1 with no heating demand in the building.

Figure 9 presents the change in the PCM's liquid fraction (the contours) along the refrigerant pipe (x-axis) during the charging period (y-axis) in a) Case 4, b) Case 5, and c) Case 1. To better understand their content, Fig. 9-b is explained more in detail. The colored lines represent the liquid fraction contours of PCM along the refrigerant pipe. After 248 min, at the end of the charging process in Case 5 and top of the y-axis of the figure, one can notice that the liquid fraction of the PCM in the first 3 m of the HX is over one. It indicates that the PCM located there is fully melted and its temperature is above its melting range. However, the rest of the PCM along the refrigerant pipe has a liquid fraction between 0.8 and 1. This indicates that the PCM located in the last 13 m of the HX is not fully melted yet and it is in the two-phase state after 248 min of the charging process.

In Case 4, the PCM is fully melted at the end of the charging period. Here, the storage unit is located downstream of the indoor unit, providing 4.5 kW of heating to the room. The two-phase refrigerant enters the storage unit, and exchanges heat with the two-phase PCM, both at a constant temperature. Thus, the enthalpy and the temperature of the PCM increase uniformly until it is fully melted. Moreover, the stored heat is totally latent heat, which is not the case for the parallel configuration. As presented in Fig. 9-b, the same amount of thermal energy is stored in the PCM, while only 19% of the material is fully melted. The stored heat is a combination of latent heat and sensible heat. In the parallel configuration, the hot gas refrigerant at the discharge temperature of the compressor enters the storage unit. It rapidly melts the PCM located at the inlet of the storage unit. While the process continues to charge the storage unit, the entrance section of the storage unit works as sensible heat storage, and its temperature increases over its melting temperature. The same phenomenon happens in the case with no heating demand in the building, as presented in Case 1 (Fig. 9-c).

The charging process of the storage unit is also investigated on occasions when the heating load in the building is very close to its designed peak load (90% of the peak). Thus, the ASHP utilizes most of its heating capacity to serve the heating load in the building. Here, in the series configuration, the outflow of the indoor unit has a very low vapor quality (around 5%). In the parallel configuration, the low mass flow rate into the storage unit causes a drastic drop in the subcooled temperature of the refrigerant. Depending on the storage size and its initial temperature, the charging process imposes a minimum heating load on the ASHP. To melt the PCM and operate with a proper subcooled degree, the heating capacity of the ASHP must be increased by raising the speed of the compressor over its nominal speed. This causes a higher work of the compressor to condition the space and melt the PCM simultaneously. The developed model simulates the occasions with high thermal load for both the series (Case 6) and the parallel (Case 7) configurations. The specifications of the simulated cases are presented in Table 3. With the augmented heating capacity, the charging period stays similar to the scenarios with a lower heating load in the building. However, the work of the compressor increases by 26% to address heating in the building and melting the PCM.

Table 3. Specifications of the cases with heating demand in the building

Simulated Cases	Building Side		ASHP Side						
	Heating load [kW]	Ratio of the peak load [%]	Configuration	Condensation T [°C]	ṁ total [kg/s]	ṁ in the storage unit [kg/s]	Storage q̇⁺ [kW]	Work of the Compressor [kW]	Charging period [min]
Case 1	0	0	Both	50	0.038	0.038	2.94	2.13	221
Case 4	4.5	60	Series	50	0.038	0.038	2.52	2.13	259
Case 5	4.5	60	Parallel	50	0.038	0.015	2.61	2.13	248
Case 6	6.75	90	Series	50	0.048	0.048	2.51	2.68	260
Case 7	6.75	90	Parallel	50	0.048	0.015	2.61	2.68	248

⁺ q̇ is the storage heat transfer rate

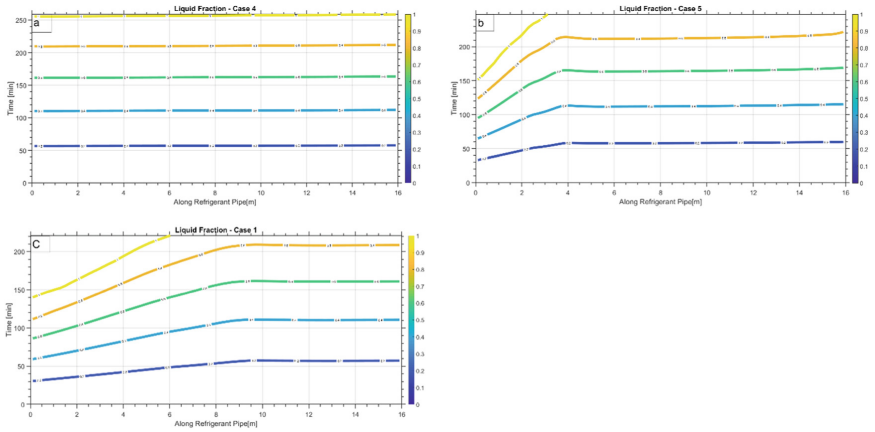

Fig. 9. PCM liquid fraction along the refrigerant pipe VS time for a) Case 4, b) Case 5, and c) Case 1

5 Conclusion and Future Works

While heat pumping technologies play a key role in the decarbonization of the built environment, their widespread adoption will significantly increase peak demand for electricity grids, especially in regions where fossil fuel-based systems are to be replaced. To address this issue, the application of a PCM as latent heat storage is investigated in ASHP systems, with a focus on residential buildings. This research proposes a new approach to integrate the storage unit as a pipe-in-pipe refrigerant/PCM HX into an ASHP. The system uses the storage unit on the load side of the HP during charging mode, while it replaces the outdoor heat exchanger during the discharging mode. Locating the storage unit on the source side during the discharge mode makes it possible to select a PCM with a neutral melting temperature, which can serve both heating and cooling applications. This study describes two possible designs of the proposed approach based

on the relative configuration of the indoor and the storage units: the series and the parallel configurations. A detailed model has also been developed to characterize numerically the effect of those configurations and building heating loads on the charging process of the storage unit. The results imply that:

- The thermal conductivity of the PCM mainly governs the heat transfer rate to the storage unit. Its relatively low thermal conduction limits the heat flux in the refrigerant/PCM HX and affects the heating capacity of the ASHP.
- By reducing the heating capacity of the ASHP, the storage unit is not charged significantly faster when there is no heating load in the building.
- On occasions with no heating demand, the system may work with a lower capacity by decreasing the compressor speed and the condensation pressure to reduce the work of the compressor. Yet, the charging period is extended longer with a lower heating capacity.
- On occasions when there is a heating load in the building, the parallel configuration charges the storage unit faster than the series configuration. Directly using the hot gas refrigerant at the discharge of the compressor creates a higher temperature difference between the refrigerant and the PCM in the storage unit, and thus a faster charging process is expected. However, the stored heat is not only latent heat. The temperature of the PCM located close to the refrigerant inlet port increases over its melting range during the charging process. In the series configuration, however, two-phase refrigerant at a constant temperature flows in the entire storage unit and melts the PCM uniformly.
- Depending on the size of the storage and its initial temperature, the charging process imposes an additional heating load on the ASHP. Therefore, the ASHP requires a higher heating capacity than its nominal capacity to charge the storage and heat the room when the thermal load on the building side is close to its peak. The compressor must operate at a higher speed to cover the increased demand. This also comes with a higher work of the compressor during the charging process.

This research work provides some initial understanding of the design of the proposed concept and the charging process. Future works are planned to further investigate the system across a full spectrum of potential operating conditions using both numerical and experimental approaches.

Acknowledgments. The authors would like to acknowledge the funding received by the Office of Energy Research and Development (OERD) of Canada through the Program of Energy Research and Development (PERD).

Authors' Contributions. Arash Bastani: Conceptualization, Methodology and Modeling, Formal Analysis, Writing - Original Draft, Visualization, Project Administration. **Justin Tamasauskas:** Conceptualization, Writing – Original Draft, Formal Analysis, Project Administration.

References

1. P. Moreno, C. Sole, A. Castell, L.F. Cabeza, The use of phase change materials in domestic heat pump and air-conditioning systems for short term storage: A review, Renew. Sustain. Energy Rev. 39 (2014) 1-13.
2. A.A. Pardinas, M.J. Alonso, R. Diz, K.H. Kvalsvik, J. Fernandez-Seara, State-of-the-art for the use of phase-change materials in tanks coupled with heat pumps, Energy and Buildings 140 (2017) 28-41.
3. F. Agyenim, N. Hewitt, Thedevelopment of a finned phase change material (PCM) storage system to take advantage of off-peak electricity tariff for improvement in cost of heat pump operation, Energy and Buildings 42 (2010), pp. 1552-1560.
4. S. Maaroui, D. Clodic, P. Dalicieux, Heat pump with a condenser including solid-liquid phase change material, International Refrigeration and Air Conditioning Conference (2012), Purdue, USA.
5. L-K. Dong, Y-Q. Jiang, Y. Yao, X-D. Zhang, Operating performance of novel reverse-cycle defrosting method based on thermal energy storage for air source heat pump, Journal of Central South University of Technology 18 (2011), pp. 2163-2169.
6. Q. Minglu, X. Liang, S. Deng, J. Yiqiang, Improved indoor thermal comfort during defrost with a novel reverse-cycle defrosting method for air source heat pumps, Building and Environment 45 (11) (2010), pp. 2354-2361.
7. M.J. Skovrup, B.D. Rasmussen, A. Jakobsen, S.E. Andersen, CoolPack tutorial Version 1.49, Department of Mechanical Engineering, Technical University of Denmark (DTU) (2011), https://www.ipu.dk/products/coolpack/
8. Y. Dutil, D.R. Rousse, N. Ben Salah, S. Lassue, L. Zalewski, A review on phase-change materials: Mathematical modeling and simulations, Renewable and Sustainable Energy Reviews 15 (2011), pp. 112–130.
9. E.W. Lemmon, I.H. Bell, M.L. Huber, M.O. McLinden, NIST Standard Reference Database 23: Reference Fluid Thermodynamic and Transport Properties-REFPROP, Version 10.0, National Institute of Standards and Technology, Standard Reference Data Program, Gaithersburg, (2018).
10. M.C. Swinton, E. Entchev, F. Szadkowski, R. Marchand, Benchmarking twin houses and assessment of the energy performance of two gas combo heating systems. Ottawa, CA: Canadian Centre for Housing Technology.
11. National Research Council of Canada. National Building Code of Canada. 13th ed. Ottawa, NRC; (2015).
12. M. Kegel, R. Sunye, J. Tamasauskas, Life Cycle Cost Comparison and Optimisation of Different Heat Pump Systems in the Canadian Climate, (2012) eSim 2012: 7th Conference of IBPSA-Canada. Halifax, Canada, paper # 1110.
13. Hydro-Quebec, Dynamic Pricing: Rate Flex D, (2020), Available at: https://www.hydroquebec.com/residential/customer-space/rates/rate-flex-d.html [Accessed Aug. 2020]